25. Renehan AG, Zwahlen M, Minder C, O'Dwyer ST, Shalet SM, Egger M. Insulin-like growth factor (IGF)-I, IGF binding protein-3, and cancer risk: systematic review and meta-regression analysis. Lancet 2004;363:1346–53.
26. Koong AC, Denko NC, Hudson KM, Schindler C, Swiersz L, Koch C, Evans S, Ibrahim H, Le QT, Terris DJ, Giaccia AJ. Candidate genes for the hypoxic tumor phenotype. Cancer Res 2000;60: 883–7.
27. Takaoka M, Harada H, Andl CD, Oyama K, Naomoto Y, Dempsey KL, Klein-Szanto AJ, El-Deiry WS, Grimberg A, Nakagawa H. Epidermal growth factor receptor regulates aberrant expression of insulin-like growth factor-binding protein 3. Cancer Res 2004;64:7711–23.
28. Hirata Y, Hayakawa H, Suzuki Y, Suzuki E, Ikenouchi H, Kohmoto O, Kimura K, Kitamura K, Eto T, Kangawa K. Mechanisms of adrenomedullin-induced vasodilation in the rat kidney. Hypertension 1995;25:790–5.
29. Udono T, Takahashi K, Nakayama M, Yoshinoya A, Totsune K, Murakami O, Durlu YK, Tamai M, Shibahara S. Induction of adrenomedullin by hypoxia in cultured retinal pigment epithelial cells. Invest Ophthalmol Vis Sci 2001;42:1080–6.
30. Le Jan S, Amy C, Cazes A, Monnot C, Lamande N, Favier J, Philippe J, Sibony M, Gasc JM, Corvol P, Germain S. Angiopoietin-like 4 is a proangiogenic factor produced during ischemia and in conventional renal cell carcinoma. Am J Pathol 2003;162:1521–8.
31. Hofbauer KH, Gess B, Lohaus C, Meyer HE, Katschinski D, Kurtz A. Oxygen tension regulates the expression of a group of procollagen hydroxylases. Eur J Biochem 2003;270:4515–22.
32. Khvatova EM, Samartzev VN, Zagoskin PP, Prudchenko IA, Mikhaleva II. Delta sleep inducing peptide (DSIP): effect on respiration activity in rat brain mitochondria and stress protective potency under experimental hypoxia. Peptides 2003;24:307–11.
33. Cangul H. Hypoxia upregulates the expression of the NDRG1 gene leading to its overexpression in various human cancers. BMC Genet 2004;5:27.
34. Szturmowicz M, Burakowski J, Tomkowski W, Sakowicz A, Filipecki S. Neuron-specific enolase in non-neoplastic lung diseases, a marker of hypoxemia? Int J Biol Markers 1998;13:150–3.
35. Denko N, Schindler C, Koong A, Laderoute K, Green C, Giaccia A. Epigenetic regulation of gene expression in cervical cancer cells by the tumor microenvironment. Clin Cancer Res 2000;6:480–7.
36. Kenny PA, Enver T, Ashworth A. Receptor and secreted targets of Wnt-1/beta-catenin signalling in mouse mammary epithelial cells. BMC Cancer 2005;5:3.
37. Fei P, Wang W, Kim SH, Wang S, Burns TF, Sax JK, Buzzai M, Dicker DT, McKenna WG, Bernhard EJ, El-Deiry WS. Bnip3L is induced by p53 under hypoxia, and its knockdown promotes tumor growth. Cancer Cell 2004;6:597–609.
38. Sowter HM, Ratcliffe PJ, Watson P, Greenberg AH, Harris AL. HIF-1-dependent regulation of hypoxic induction of the cell death factors BNIP3 and NIX in human tumors. Cancer Res 2001;61: 6669–73.

Oncogene (2006) 25, 5994–6002
© 2006 Nature Publishing Group All rights reserved 0950-9232/06 $30.00
www.nature.com/onc

ORIGINAL ARTICLE

Identification of expressed genes characterizing long-term survival in malignant glioma patients

R Yamanaka[1], T Arao[2], N Yajima[1], N Tsuchiya[1], J Homma[1], R Tanaka[1], M Sano[1], A Oide[3], M Sekijima[3] and K Nishio[2]

[1]*Department of Neurosurgery, Brain Research Institute, Niigata University, Niigata City, Japan;* [2]*Pharmacology Division, National Cancer Center Research Institute, Chuo-ku, Tokyo, Japan and* [3]*Mitsubishi Chemical Safety Institute, Ibaraki, Japan*

Better understanding of the underlying biology of malignant gliomas is critical for the development of early detection strategies and new therapeutics. This study aimed to define genes associated with survival. We investigated whether genes coupled with a class prediction model could be used to define subgroups of high-grade gliomas in a more objective manner than standard pathology. RNAs from 29 malignant gliomas were analysed using Agilent microarrays. We identified 21 genes whose expression was most strongly and consistently related to patient survival based on univariate proportional hazards models. In six out of 10 genes, changes in gene expression were validated by quantitative real-time PCR. After adjusting for clinical covariates based on a multivariate analysis, we finally obtained a statistical significance level for *DDR1* (discoidin domain receptor family, member 1), *DYRK3* (dual-specificity tyrosine-(Y)-phosphorylation-regulated kinase 3) and *KSP37* (Ksp37 protein). In independent samples, it was confirmed that DDR1 protein expression was also correlated to the prognosis of glioma patients detected by immunohistochemical staining. Furthermore, we analysed the efficacy of the short interfering RNA (siRNA)-mediated inhibition of DDR1 mRNA synthesis in glioma cell lines. Cell proliferation and invasion were significantly suppressed by siRNA against DDR1. Thus, DDR1 can be a novel molecular target of therapy as well as an important predictive marker for survival in patients with glioma. Our method was effective at classifying high-grade gliomas objectively, and provided a more accurate predictor of prognosis than histological grading.
Oncogene (2006) **25**, 5994–6002. doi:10.1038/sj.onc.1209585; published online 1 May 2006

Keywords: cDNA array; gene expression profiles; glioma; survival predictor; siRNA

Correspondence: Dr R Yamanaka, Department of Neurosurgery, Brain Research Institute, Niigata University, Asahimachi-dori 1-757, Niigata City 951-8585, Japan.
E-mail: ryaman@bri.niigata-u.ac.jp
Received 7 November 2005; revised 8 March 2006; accepted 8 March 2006; published online 1 May 2006

Introduction

Glioblastoma, which is pathologically the most aggressive form, has a median survival range of only 9–15 months (Karpeh *et al.*, 2001; Stewart, 2002; Stupp *et al.*, 2005). Advances in the basic knowledge of cancer biology and surgical techniques, chemotherapy and radiotherapy have led to little improvement in the survival rates of patients suffering from glioblastoma (Stewart, 2002). Poor prognosis is attributable to difficulties of early detection, and to a high recurrence rate during post-initial treatment observation periods. Therefore, it is important to devise more effective therapeutic approaches, to reveal more clearly the biological features of glioblastoma, and identify novel target molecules for diagnosis and therapy of the disease. Several histological grading schemes exist, but the two-tiered World Health Organization (WHO) system is currently the most widely used (Kleihues and Cavenee, 2000). A high WHO grade correlates with clinical progression and decreased survival. However, there are still many individual variabilities within diagnostic categories, leading to the need for developing additional prognostic markers. As prognostic markers are based on morphology, identification of new treatment strategies is limited. Identification of distinct molecular pathways has become critical for developing molecular targeted therapies.

Recently, developed microarray technology has permitted development of multi-organ cancer classification including gliomas (Ramaswamy *et al.*, 2001; Rickman *et al.*, 2001; Kim *et al.*, 2002; Hunter *et al.*, 2003; Mischel *et al.*, 2004), identification of tumor subclasses (Khan *et al.*, 2001; Mischel *et al.*, 2003; Shai *et al.*, 2003; Sorlie *et al.*, 2003; Liang *et al.*, 2005; Nigro *et al.*, 2005; Wong *et al.*, 2005), discovery of progression markers (Sallinen *et al.*, 2000; Agrawal *et al.*, 2002; van de Boom *et al.*, 2003; Godard *et al.*, 2003; Hoelzinger *et al.*, 2005; Rich *et al.*, 2005; Somasundaram *et al.*, 2005) and prediction of disease outcomes (van't Veer *et al.*, 2002; van de Vijver *et al.*, 2002; Nutt *et al.*, 2003; Freije *et al.*, 2004). Unlike clinicopathological staging, molecular staging can predict long-term outcomes of any individual based on gene expression profile of the tumor at diagnosis. Analysis of expression profiles of genes in

clinical materials is an essential step toward clarifying the detailed mechanisms of oncogenesis and discovering target molecules for the development of novel therapeutic drugs.

The human 1 cDNA microarray (Agilent Technologies, Palo Alto, CA, USA) contains 12811 clones from more than 7000 UniGene clusters. Each clone is represented by a PCR-amplified, double-stranded complementary DNA (cDNA) product, immobilized on the slide. mRNAs obtained from two biological samples were separately converted to cDNA labeled with distinct fluorescent dyes, usually cyanines 3 (Cy3) and 5 (Cy5), mixed together and hybridized to a single array. Hybridization intensities from the two dyes were measured, and compared for each gene within the array, to identify gene expression differences between the two samples. Utilization of a common reference sample for each array allowed objective comparisons between samples on separate arrays. In the present study, we used agilent cDNA microarrays to define expression patterns to distinguish between short-term and long-term survival of malignant gliomas.

Results

High-grade gliomas in this study

Patients initially showed histologically proven glioblastoma (grade IV), anaplastic astrocytoma or other malignant gliomas (grade III) corresponding to the WHO criteria. Seven patients with grade III and 22 patients with grade IV were included in this study (Table 1). Univariate analysis of clinical features was performed against pathological diagnoses, age, gender and performance status (PS) with respect to survival. Pathological diagnoses, age and gender were not independent predictors of survival (Table 2). Once all gliomas were sorted according to PS, significant difference was found between survival of patients with PS 0–60 and patients with PS 70–100 in our cases (Table 2).

Identification of prognosis-related genes

We performed the univariate proportional hazard model to identify a set of genes that better correlated with censored survival time. Genes were selected if their *P*-value was less than 0.005 and the *P*-value was then used in a multivariate permutation test. We identified 21 genes whose expression was most strongly and consistently related to survival. These genes are listed in Table 3, and include several genes that we believe to be biologically active such as DDR1 (discoidin domain receptor family, member 1) and KSP37 (Ksp37 protein) (see Discussion).

Relationships between results obtained by microarray analysis and by real-time PCR

We chose 10 genes that were not previously associated with gliomas, to measure their mRNA levels by real-time quantitative reverse transcription–PCR. From 29 microarray-measured tumor samples, total RNAs from 27 tumor samples (14 long-term survivors and 13 short-term survivors) were analysed for expressions of ALCAM (activated leukocyte cell adhesion molecule), DDR1, DYRK3 (dual-specificity tyrosine-(Y)-phosphorylation-regulated kinase 3), ITGA5 (integrin alpha 5), ITGB2 (integrin beta 2), KSP37, LDHC (lactate dehydrogenase C), LOC (hypothetical protein

Table 1 Patient characteristics

No.	*Histological diagnosis*	*Age, gender*	*WHO grade*	*PS*	*Survival time*
1	Anaplastic oligoastrocytoma	59, M	III	80	263
2	Anaplastic oligodendroglioma	60, M	III	90	294
3	Anaplastic oligodendroglioma	72, M	III	90	305
4	Anaplastic astrocytoma	32, M	III	100	545
5	Anaplastic astrocytoma	73, M	III	70	617
6	Anaplastic astrocytoma	45, M	III	60	698
7	Anaplastic astrocytoma	65, M	III	90	762
8	Glioblastoma	18, F	IV	60	111
9	Glioblastoma	64, F	IV	50	154
10	Glioblastoma	28, M	IV	70	202
11	Glioblastoma	45, M	IV	60	261
12	Glioblastoma	54, M	IV	40	268
13	Glioblastoma	68, M	IV	80	286
14	Glioblastoma	62, M	IV	70	347
15	Glioblastoma	80, M	IV	80	349
16	Glioblastoma	78, F	IV	60	350
17	Glioblastoma	69, M	IV	90	352
18	Glioblastoma	67, M	IV	50	396
19	Glioblastoma	63, M	IV	60	405
20	Glioblastoma	20, F	IV	90	417
21	Glioblastoma	71, M	IV	80	436
22	Glioblastoma	31, M	IV	90	453
23	Glioblastoma	56, M	IV	80	506
24	Glioblastoma	55, M	IV	80	630
25	Glioblastoma	52, F	IV	90	641
26	Glioblastoma	27, F	IV	90	757
27	Glioblastoma	42, F	IV	70	880
28	Glioblastoma	47, M	IV	90	908
29	Glioblastoma	42, M	IV	90	1189

Abbreviation: PS, performance status; WHO, World Health Organization.

Table 2 Univariate analysis of clinical features

Variable	*No. of patients*	*Median survival time (days)*	P *(log-rank test)*
WHO grade			
Grade III	7	617	0.56
Grade IV	22	417	
Age (years)			
<60	16	641	0.069
⩾60	13	352	
Gender			
Male	22	436	0.979
Female	7	417	
PS			
70–100	21	617	0.0033
0–60	8	309	

Abbreviation: PS, performance status; WHO, World Health Organization.

Table 3 Identification of prognosis-related genes

GenBank	*Symbol*	*Description*	*Hazard ratio*	P-*value*
BC005261	SLN	Sarcolipin	0.41	0.000263
U13680	LDHC	Lactate dehydrogenase-C	0.24	0.000851
AL1 37662	NRBP2	Nuclear receptor binding protein 2	5.5	0.00101
AB021123	KSP37	Ksp37 protein	0.12	0.00102
M20681	GLUT3	Glucose transporter-like protein-III	0.37	0.00107
BC007952	PKM2	Pyruvate kinase, muscle	0.15	0.0013
N92498	PDCD4	Programmed cell death 4	3.1	0.00205
M10036	TPI1	Triosephosphate isomerase 1	0.16	0.00222
BC015061	RAB32	RAB32, member RAS oncogene family	0.51	0.00260
U20362	TTC10	Intraflagellar transport 88 homolog	4.5	0.00290
BE045190	DDR1	Discoidin domain receptor family, member 1	4.2	0.00308
AF327561	DYRK3	Dual-specificity tyrosine-(Y)-phosphorylation regulated kinase 5	0.17	0.00312
BC005861	ITGB2	Integrin, beta 2	4.1	0.00352
BAB22510		Putative	8.0	0.00365
BC007835	STK40	Serine/threonine kinase 40	0.40	0.00369
AB026706	EMILIN2	Elastin microfibril interfacer 2	0.27	0.00389
AF231512	RBM8B	RNA binding motif protein 8B	4.3	0.00403
BC008786	ITGA5	Integrin, alpha 5	0.36	0.00419
AA404652	ISGF3G	Interferon-stimulated transcription factor 3, gamma (48 kD)	2.8	0.00431
Y10183	ALCAM	Activated leukocyte cell adhesion molecule	2.8	0.00440
MI 9482	ATP synthase	Human ATP synthase beta subunit gene, exons 1–7	0.28	0.00445

A subset of the 21 genes expressed differentially in good and poor prognosis group, listed by category. Included with name of each gene is the GeneBank accession number, a brief description of the gene and the *P*-value that was computed.

Table 4 mRNA levels by real-time quantitative RT–PCR

	Short-term survivor (n = 13)	*Long-term survivor (n = 14)*	P
ALCAM (ng/ml)	6.6±14.5	0.06±0.1	<0.05
DDR1 (pg/ml)	416.8±56.5	40.6±11.1	<0.01
DYRK3 (ng/ml)	116.1±96.2	449.3±108.7	<0.05
ITGA5 (pg/ml)	38.7±47.1	707.6±85.6	<0.01
ITGB2 (pg/ml)	0.02±0.01	0.03±0.05	NS
KSP37 (pg/ml)	18.9±24.6	8402.9±855.6	<0.01
LDHC (pg/ml)	1.4±1.0	7.5±12.5	NS
LOC (pg/ml)	1.2±1.1	1.7±2.1	NS
SLN (pg/ml)	8.9±1.9	15.5±4.5	<0.05
SLC2A3 (ng/ml)	7.5±8.3	19.1±23.9	NS

Abbreviations: NS, not significant; RT-PCR, reverse transcription–PCR. For other abbreviations, see Table 3.

Table 5 Multivariate analysis

Variable	*Hazard ratio*	*95% CI*	P
WHO grade	9.55	1.24–73.8	0.0305
Age (⩾60)	5.88	1.1–31.4	0.038
Gender (male)	8.16	0.748–88.9	0.0851
PS (70–100)	18.2	2.47–134	0.0044
DDR1	21.5	2.12–217	0.0094
DYRK3	0.067	0.006–0.798	0.0325
KSP37	0.008	0.000–0.235	0.0053
ITGA5	0.698	0.146–3.34	0.6525
SLN	2.85	0.658–12.4	0.1615
ALCAM	1.67	0.446–6.274	0.4453

Abbreviations: CI, confidence interval; PS, performance status; WHO, World Health Organization. For other abbreviations see Table 3.

LOC340371), SLN (sarcolipin) and SLC2A3 (solute carrier family 2 member 3). Results are shown in Table 4, and are expressed as means±standard deviation (s.d.). Patterns of gene expression between long- and short-term survivors analysed by microarray paralleled patterns observed using real-time PCR for ALCAM, DDR1, DYRK3, ITGA5, KSP37 and SLN (Table 3).

DDR1, DYRK3 and KSP37 were selected based on a multivariate analysis

To adjust for relevant clinical covariates against six PCR-confirmed genes, we performed a multivariate analysis (Table 5). In incorporating multivariate analysis, high DDR1 expression was negatively correlated with survival ($P=0.0094$; hazard ratio = 21.5; 95% confidence interval (CI), 2.12–217), high DYRK3 expression was positively correlated with survival ($P=0.0325$; hazard ratio = 0.067; 95% CI, 0.006–0.798) and high KSP37 expression was positively correlated with survival ($P=0.0053$; hazard ratio = 0.008; 95% CI, 0.000–0.235). The expression of DDR1 and KSP37 were more closely correlated with survival compared to histological grade (Table 5). Thus, in gliomas, these results suggested that expression of *DDR1*, *DYRK3* and *KSP37* might be a strong predictive factor for patient's survival better than WHO grading.

Immunohistochemical analysis of potential candidate genes

To confirm our results from microarray analysis, we chose to investigate DDR1 expression as a prognostic marker for glioma and performed the immunohistochemical analysis. Firstly, we analysed the protein expression of DDR1 against 29 microarray-measured specimens, and investigated the correlations with patient survivals. DDR1 was expressed in the cytoplasm of neoplastic cells and patients were divided into two

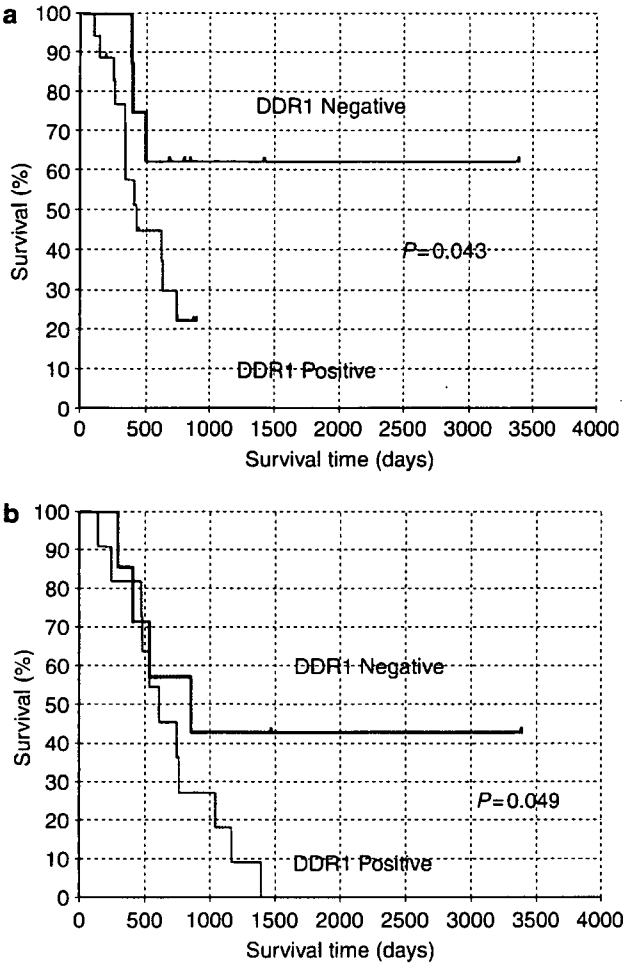

Figure 1 DDR1 protein expressions and patient survivals. Kaplan–Meier survival curves for patients, stratified according to levels of DDR1 expressions in tumors (low DDR1 staining: 0–1 score; high DDR1 staining: 2–3 score; log-rank test). (**a**) A significant trend for worse outcome was observed in the DDR1-positive group ($P=0.043$). (**b**) DDR1 protein expressions and patient survivals in independent groups of gliomas. Kaplan–Meier survival curves for patients, stratified according to levels of DDR1 expressions in tumors (low DDR1 staining: 0–1 score; high DDR1 staining: 2–3 score; log-rank test). A significant trend for worse outcome was observed in the DDR1-positive group ($P=0.049$).

groups: positive and negative groups according to immunostaining score. Positive staining for DDR1 was confirmed to be associated with unfavorable overall survival time ($P=0.043$; Figure 1a). Next, in new independent 19 glioma samples, similar results were obtained ($P=0.049$; Figure 1b). Although our results were based on relatively small sample size, the correlation between DDR expression and survival was confirmed by real-time quantitative PCR and also confirmed immunohistochemical analysis in independent samples.

Glioma cell proliferation and invasion are inhibited by DDR1 siRNA

DDR1 overexpression was linked to aggressiveness of glioma in our analysis. In order to determine whether downregulation of endogenous DDR1 suppresses proliferation and invasive behavior of gliomas, we synthesized short interfering RNA (siRNAs) against DDR1 mRNA to reduce expression of DDR1 protein. We analysed efficacy of siRNA-mediated inhibition of DDR1 mRNA synthesis in U251, GI-1, and T98G cells by real-time PCR. As shown in Figure 2a, when U251 cells were transfected with siRNAs against DDR-1 (DDR1-#1 and DDR1-#2), DDR1 mRNA was downregulated 48 h later ($P<0.01$), whereas transfection with a related control siRNA failed to modify DDR1 mRNA expression. When GI-1 and T98G cells were transfected with siRNAs against DDR-1 (DDR1-#1 and DDR1-#2), DDR1 mRNA was downregulated by 10–15% of control siRNA ($P<0.01$).

After transfection with siRNAs against DDR-1, U251 cell counts within 48 h were approximately 40–60% of untreated or control-siRNA-treated cells during this same period of time ($P<0.01$; Figure 2b). GI-1 and T98G cell counts within 48 h were approximately 35–50% of untreated or control-siRNA-treated cells during this same period of time ($P<0.01$). Cell proliferation was significantly suppressed by siRNA against DDR1, as reflected in reduction of mRNA expression.

For invasion assays, transfectants were seeded onto Matrigel-coated invasion chambers, incubated for 24 h and total numbers of cells on the underside of each filter were determined. As shown in Figure 2c, transfections of U251 cells with anti-DDR1 siRNA inhibited cell invasion through the Matrigel by more than 80%, whereas the use of control siRNA had no effect ($P<0.01$). Transfections of GI-1 and T98G cells with anti-DDR1 siRNA inhibited cell invasion through the Matrigel by more than 70–80%, whereas the use of control siRNA had no effect ($P<0.01$). Therefore, invasion by cells was significantly suppressed by siRNA against DDR1, as reflected by reduced mRNA expression.

Discussion

Several works (Sallinen *et al*., 2000; Khan *et al*., 2001; Ramaswamy *et al*., 2001; Rickman *et al*., 2001; Agrawal *et al*., 2002; Kim *et al*., 2002; Veer *et al*., 2002; Vijver *et al*., 2002; Boom *et al*., 2003; Godard *et al*., 2003; Hunter *et al*., 2003; Mischel *et al*., 2003; Nutt *et al*., 2003; Shai *et al*., 2003; Sorlie *et al*., 2003; Freije *et al*., 2004; Mischel *et al*., 2004; Hoelzinger *et al*., 2005; Liang *et al*., 2005; Nigro *et al*., 2005; Rich *et al*., 2005; Somasundaram *et al*, 2005; Wong *et al*., 2005) showed the usefulness of utilizing methods of analysis of multiple forms of data including both clinical and multiple genes, to achieve a more precise discrimination of outcomes for individual patients. The same logical use of multiple forms of data and methods of analysis has been applied in the present study to accurately achieve better classification and prediction of glioma patients. In the present study, we used expression arrays to identify genes that reflect patient's survival. The groups of patients used represented the two extremes of

glioma with respect to outcomes. Nutt *et al.* (2003) and Freije *et al.* (2004) reported the use of microarrays to predict outcomes for glioma patient. Nutt *et al.* involved a group of 50 glioma patients who were not selected based on survival duration. The investigators used Affymetrix U 95 GeneChips to develop a model to classify cases into unfavorable and favorable groups that exhibited significantly different survivals. They picked up 20 genes different from our study that highly correlated with class distinction. On the other hand, Freije *et al.* (2004) also reported the use of microarrays to predict outcomes for all histological types of 85 gliomas. The investigators used Affymetrix HG 133 GeneChips to develop a 44-gene model to classify cases into unfavorable and favorable groups that exhibited significantly different survivals. From these two studies, there were no attempt to predict survivals of individual patients, but results were consistent with ours, and together suggested that clinical differences in outcomes were reflected in global patterns of gene expression that could be appreciated using microarrays.

Some of the genes that were critical components of patterns that were used to discriminate between long-term and short-term survivors are known to affect virulence of the malignant phenotype. Several groups have confirmed prognostic markers of glioma such as Insulin-like growth factor-binding protein 2 (IGFBP2) (Kim *et al.*, 2002; Godard *et al.*, 2003), vascular endothelial growrh factor (VEGF) (Godard *et al.*, 2003), Osteonectin, Doublecortex, Semaphorin 3B (Rich *et al.*, 2005) and brain-type fatty acid-binding protein (FABP7) (Liang *et al.*, 2005).

We have selected *DDR1*, *KSP37* and *DYRK3* from a 21-gene model (21 genes derived from multivariate analysis) to classify cases into unfavorable and favorable groups that exhibited significantly different survivals. We observed that glioma cell proliferation and invasion were significantly suppressed by siRNA against DDR1. The DDR1 is a tyrosine receptor kinase activated by various types of collagen, and is involved in cell–matrix communication (Vogel, 1999). DDR1 is activated independently of β1 integrin (Vogel *et al.*, 2000). DDR1–collagen interaction facilitates the adhesion, migration, differentiation/maturation and cytokine/chemokine production of leukocytes (Yoshimura *et al.*, 2005). DDR1 is overexpressed in several tumors including high-grade brain, esophageal and breast cancers (Weiner and Zagzag, 2000). Based on our data and Ram *et al.* (2005), DDR1 may play a potential role in proliferation and invasion of gliomas. Invasive phenotype is caused by activation of matrix metalloproteinase-2 in DDR1-overexpressing cells (Ram *et al.*, 2006). Glioma cell adhesion, including intercellular and

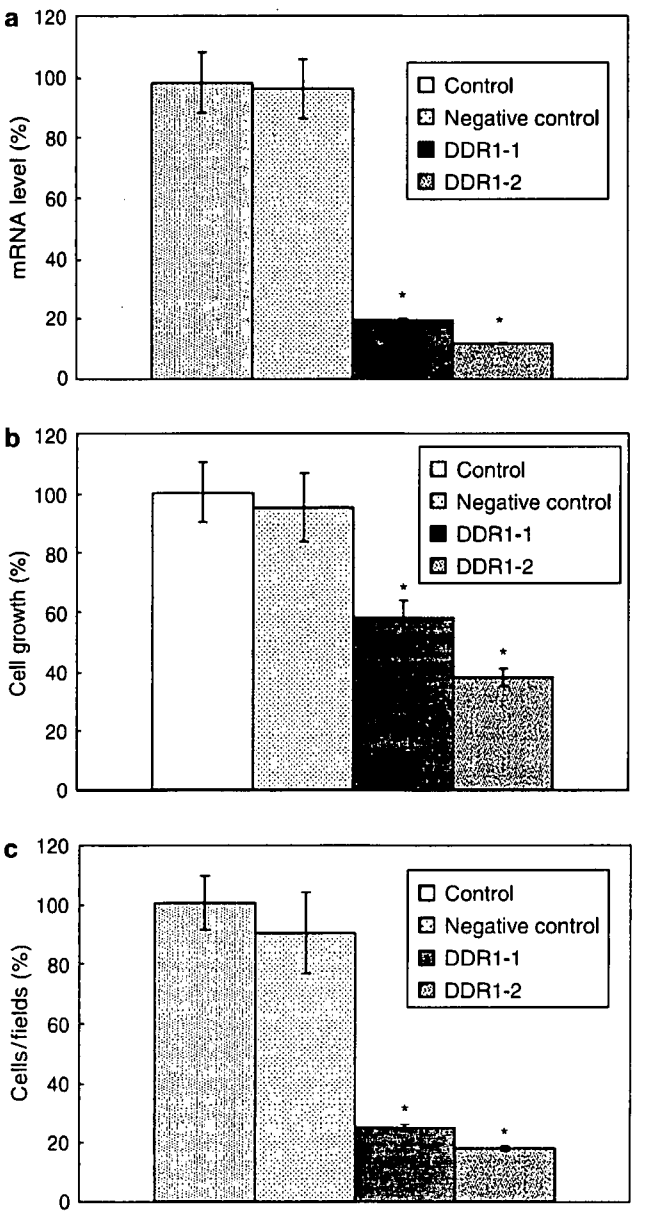

Figure 2 Effects of DDR1 knockdown by RNA interference on proliferation and invasiveness of human glioma cell lines. U251 cells were transiently transfected with short interfering RNAs (siRNA) and subjected to semiquantitative PCR analysis, proliferation assay or Matrigel invasion assays. (**a**) Reduction of DDR1 mRNA expression by siRNAs against DDR1 was determined by semiquantitative PCR analysis. Transfection with DDR1 siRNAs significantly reduced DDR1, whereas transfection with siRNAs targeted to an unrelated mRNA had no effect on DDR1 expression. $^{*}P<0.01$ compared with both control groups. (**b**) Cell proliferation assay. Cells were cultured in 96-well plates in 100 μl of serum-enriched medium. When 80% confluence was reached, 25 μl of 100 nM siRNA in cytofectin was added drop wise. Numbers of viable cells were evaluated after 48 h culture by incubation with Tetra color one, and numbers obtained were compared with those of controls. After transfection with DDR1 siRNAs, U251 cell counts within 48 h were approximately 40–60% of untreated or control-siRNA-treated cells during this same period of time. $^{*}P<0.01$ compared with both control groups. (**c**) For the invasion assays, transfectants were seeded onto Matrigel-coated invasion chambers and incubated for 24 h. Total numbers of cells on the underside of each filter were determined. Invading cells were significantly suppressed by siRNAs against DDR1, as reflected by reduction of mRNA expression. Control, no siRNA treatment; negative control, control siRNA treated. DDR1-#1, DDR1-#2; DDR1 siRNA treated. $^{**}P<0.01$ compared with both control groups.

cell–matrix adhesions, is critical to the maintenance of structural integrity, polarity and cell–cell communication, and their expression is frequently observed in tumor cells concordant with a breakdown of cellular organization, causing an uncontrolled leakage of nutrients and other factors necessary for the survival and growth of tumor cells, and loss of cell–cell contact inhibition leading to increased cell motility. Thus, DDR1 may be a novel molecular target for therapy, and provide an important predictive marker for survival in patients with glioma. KSP37 protein is constitutively secreted by Th1-type CD4-positive lymphocytes and lymphocytes with cytotoxic potential, and may be involved in an essential process of cytotoxic lymphocyte-mediated immunity (Ogawa *et al.*, 2001). Down-regulation of KSP37 protein may correlate with poor prognosis of glioma patients with immunosuppressive state. DYRK3 is a member of dual-specificity tyrosine-regulated kinases with roles in cell growth and development. DYRK3 was reported to be expressed in erythroid progenitor cells, and to play roles in kinase activation (Li *et al.*, 2002). Although KSP37 and DYRK3 are unique molecules, their roles in glioma progression are unclear, and should be further investigated in the future.

Regardless of their roles in tumorigenesis, all these markers offer potential clinical applications for the treatment and detection of malignant gliomas. To our knowledge, this study is the first to address these molecules as molecular targets for therapeutics. Values of gene-expression-based predictors for prognosis of malignant glioma patients will not be fully realized until additional therapies are available for patients destined to have poor survival, following conventional chemotherapy. In this regard, expression profiles may not only predict the likelihood of long-term survival following nitrosourea chemotherapy, but may also yield clues on individual genes involved in tumor development, progression and response to therapy. It is likely that some of the most differentially expressed genes such as those discussed above will represent therapeutic molecular targets. Moreover, the ability to histologically distinguish ambiguous gliomas will enable appropriate therapies to be tailored to specific tumor subtypes. Class prediction models based on defined molecular profiles allow classification of malignant gliomas in a manner that will better correlate with clinical outcomes than with standard pathology.

Materials and methods

Patients

Mean age of patients was 53.2 years old (range, 18–80). Twenty-two patients were men and seven were women. Tissues were snap-frozen in liquid nitrogen within 5 min of harvesting, and stored thereafter at −80°C. Clinical stage was estimated from accompanying surgical pathology and clinical reports. Samples were specifically re-reviewed by a board-certified pathologist in our institution, using observation of sections of paraffin-embedded tissues that were adjacent or in close proximity to the frozen sample from which the RNA was extracted. Histopathology of each collected specimen was reviewed to confirm adequacy of the sample (i.e., minimal contamination with non-neoplastic elements), and to assess the extent of tumoral necrosis and cellularity. Histological characteristics of tumor samples and clinical disease stage were included as supplements in Table 1.

After surgical resection of tumor, patients had a course of external beam radiation therapy (standard dose of 40 Gy to the tumor with a 3-cm margin, and 20 Gy boost to the whole brain) and nitrosourea-based chemotherapy. Patients were monitored for recurrences of tumor during the initial and maintenance therapy by magnetic resonance imaging or computed tomography. Treatments were carried out at the Department of Neurosurgery, Niigata University Hospital. Informed consent was obtained from all patients for the use of samples in accordance with the guidelines of the Ethical Committee on Human Research, Niigata University Medical School. Overall survival was measured from the date of diagnosis. Survival end points corresponded to dates of death or last follow-up.

RNA extraction

Total RNA was extracted with 1 ml Isogen (Nippongene, Toyama, Japan) per 100 mg frozen glioma tissues, following the manufacturer's instructions. Each tissue type was homogenized with a Polytron (Fisher Scientific) for 30 s and cleared by a 10-min centrifugation at 10 000 *g*. For each ml Isogen, 0.2 ml chloroform was added and samples were vigorously shaken for 20 s and then incubated on ice for 10 min. The aqueous phase was separated by centrifugation at 10 000 *g* for 10 min, decanted and an equal volume of isopropanol was added. The mixture was allowed to precipitate for 10 min and the precipitate was collected by centrifugation at 12 000 *g* for 10 min. The pellet was washed with 70% ethanol, collected by brief centrifugation, air dried and re-suspended in H_2O. RNA was further purified using an RNeasy column (Qiagen, Valencia, CA, USA). The purified RNA was quantified using a UV spectrophotometer, and RNA quality was evaluated by capillary electrophoresis on an Agilent 2100 Bioanalyzer (Agilent Technologies). Only samples with 28S/18S ratios >0.7 and with no evidence of ribosomal peak degradation were included in the study.

Agilent cDNA microarrays

Agilent human 1 cDNA microarrays (Agilent Technologies) contained 13 156 clones from Incyte's human cDNA library. Test and normal brain RNAs were labeled with both Cy3-dCTP and Cy5-dCTP nucleotides (Amersham Biosciences, Tokyo, Japan) and hybridized on two slides (dye-swap hybridizations) according to the direct-labeling method provided by the manufacturer. Following hybridization, slides were scanned and analysed using the Feature Extraction software (version A.4.0.45, Agilent Technologies), as recommended by the manufacturer. Spots that did not pass quality control procedures in the Feature Extraction software were flagged and removed from further analysis. Clones with the same GenBank accession number were averaged.

Expression profiling on Agilent cDNA microarrays

Total RNA (20 μg) was reverse transcribed using the Agilent direct-label cDNA synthesis kit (Agilent Technologies), following the manufacturer's directions. Labeled cDNA was purified using QIAquick PCR Purification columns (Qiagen, Valencia, CA, USA), followed by concentration by vacuum centrifugation. cDNA was suspended in hybridization buffer and hybridized to Agilent human 1 cDNA microarrays (Agilent Technologies) for 17 h at 65°C, according to the

Agilent protocol. To avoid generation of false between-group differences by randomly pairing glioma samples on the two-channel cDNA arrays, each sample was individually labeled and co-hybridized with a normal brain sample labeled with a complementary dye. Normal brain samples were generated by pooling equal amounts of RNA from each control sample and labeling as for individual samples. In addition, Cy dye switch hybridizations were performed for each sample. Normal brain samples were purchased from Clontech (Tokyo, Japan). All microarray data and clinical features have been submitted to Gene Expression Omnibus (GEO, http://www.ncbi.nlm.nih.gov/geo; accession no. GSE4381).

Statistical analysis

Univariate analysis for clinical features was performed by log-rank test using SAS software ver. 9.1.3 (SAS Institute Inc., Cary, NC, USA). In microarray analysis, normalization and survival analysis were performed using the BRB Array Tools software ver. 3.3.0 (http://linus.nci.nih.gov/BRB-ArrayTools.html) developed by Dr Richard Simon and Amy Peng. In brief, a log base 2 transformation was applied to the microarray raw data, and global normalization was used to median the center of log ratios on each array in order to adjust for differences in labeling intensities of the Cy3 and Cy5 dyes. Genes showing minimal variation across the set of arrays were excluded from the analysis. Genes whose expression differed by at least 1.5-fold from the median in at least 20% of the arrays were retained. Genes were also excluded if percent of data missing or filtered out exceeds 50%. Then, genes that passed filtering criteria were considered for further analysis.

We computed a statistical significance level for each gene based on univariate proportional hazards models ($P<0.005$) and identified genes whose expression was significantly related to survival of the patient. These P-values were then used in a multivariate permutation test in which survival times and censoring indicators were randomly permuted among arrays. To adjust the expression of six candidate genes (DDR1, DYRK3, KSP37, ITGA5, SLN and ALCAM) for clinical features (WHO grade, age, gender, PS), clinical data and normalized microarray expression data of six genes were imported into SAS software ver. 9.1.3 (SAS Institute Inc.) and Cox regression model was performed for multivariate analysis against each variable (WHO grade, age, gender, PS, expression levels of six genes). Three samples were excluded for multivariate analysis because there were a few defected expression data. A P-value <0.05 was considered significant. The differences between subgroups of DDR1 siRNA and control groups were tested for statistical significance using the analysis of variance test and statistical significance was determined at the $P<0.01$ level.

Validation of differential expression by real-time quantitative PCR

Total RNA (2 μg) was subjected to DNase treatment in a 10 μl reaction containing 1 μl 10 × DNase I reaction buffer (Invitrogen, Tokyo, Japan) and 1 μg DNase I at room temperature for 10 min. Ethylenediamine tetraacetic acid (1 μl, 25 mM) and 1 μl oligo dT (0.5 μg/μl; Invitrogen) were added to the DNase reaction, and heated to 70°C for 15 min to inactivate DNase I activity and eliminate RNA secondary structure. Samples were placed on ice for 2 min and collected by brief centrifugation. RNA was then reverse-transcribed into cDNA by adding 8 μl master mix containing 4 μl of 5 × first strand buffer, 2 μl dithiothreitol (0.1 M), 1 μl dNTPs (10 mM each) and 1 μl SuperScript II (200 U/μl) (Invitrogen), followed by incubation at 42°C for 45 min. The reaction was diluted 10-fold with dH_2O and stored at 4°C.

Each sample was subjected to 40 cycles of real-time PCR with a LightCycler (Idaho Technology, Salt Lake City, UT, USA). PCR reagents contained 1 × LightCycler DNA Master SYBR Green I (Roche Molecular Biochemicals, Mannheim, Germany), 0.5 μM of each primer, 3 mM $MgCl_2$ and 2 μl cDNA template. PCR conditions were as follows: one cycle of denaturing at 95°C for 10 min, followed by 40 cycles of 95°C for 15 s, 55°C for 5 s and 72°C for 10 s. A melting curve was obtained at the end of amplification cycles to verify specificity of the PCR products. Points at which signal fluorescence exceeded background, for each sample and for each gene, were compared to a standard curve generated by four, 10-fold serial dilutions of concentrated cDNA control of each sample subjected to real-time analysis to determine an expression value. All determinations were performed in duplicate. A Student's t-test was conducted to analyse expression values for long- and short-term survivors to determine statistical significance. For amplification of target genes, the following primers were used (Takara, Yotsukaichi, Japan):

ALCAM-FW:	5′-CCAGATGGCAATATCACATGGTACA-3′,
ALCAM-RW:	5′TCCAGGGTGGAAGTCATGGTATAGA-3′,
DDR1-FW:	5′ACTTTGGCATGAGCCGGAAC-3′,
DDR1-RW:	5′ACGTCACTCGCAGTCGTGAAC-3′,
DYRK3-FW:	5′AGCTGCCTCCAGTTGTTGGGAATAG-3′,
DYRK3-RW:	5′TGCATCTCTGGGCATATCTCTGTC-3′,
ITGA5-FW:	5′TCCCAGTAAGCGACTGGCATC-3′,
ITGA5-RW:	5′GTTCCAGCACACCCTGGCTAA-3′,
ITGB2-FW:	5′ATCGTGCTGATCGGCATTCTC-3′,
ITGB2-RW:	5′GGTTCATGACCGTCGTGGTG-3′,
KSP37-FW:	5′CTTCCGAGGGTGACAGGTGA-3′,
KSP37-RW:	5′TCCAGTGTGAGAACGTTGGATTG-3′,
LDHC-FW:	5′TCATCTGTACTGATTGCGCCAAG-3′,
LDHC-RW:	5′ACGGCACCAGTTCCAACAATAGTAA-3′,
LOC340371-FW:	5′GGAACATGCCAGGGCTTCA-3′,
LOC340371-RW:	5′CTGCTCAACACGGTCTGGA-3′,
SLN-FW:	5′GGAGTTGGAGCTCAAGTTGGAGAC-3′,
SLN-RW:	5′GAACTGCAGGCAGATTTCTGAGG-3′,
SLC2A3-FW:	5′GCCTTTGGCACTCTCAACCAG-3′,
SLC2A3-RW:	5′GCTGCACTTTGTAGGATAGCAGGAA-3′.

Immunohistochemistry

Sections (5 μm) from formalin-fixed, paraffin-embedded tissue specimens were deparaffinized in xylene and dehydrated in a graded series of ethanol, followed by a phosphate-buffered saline (PBS) wash. Antigen retrieval was carried out by incubation at 121°C for 10 min in 10 mM sodium citrate (pH 6.0), followed by incubation with 0.3% H_2O_2 to quench endogenous peroxidase activity. Slides were blocked in 10% normal serum and incubated with rabbit polyclonal anti-DDR1 antibody (dilution 1:50; Santa Cruz Biotechnology, Santa Cruz, CA, USA) for 16 h at 4°C. After washing, the slides were incubated with an avidin–biotin–peroxidase system (Vectastain elite ABC kit, Vector Labs, Burlingame, CA,

USA). Finally, sections were exposed for 10–20 min to 0.01% 3,3-diaminobenzidine (Sigma, Tokyo, Japan) and PBS containing 0.01% hydrogen peroxide. Immunohistochemistry scoring was performed as follows. Staining intensity was classified as none (0 point), weak (1 point), moderate (2 point) or strong (3 point). Intensity of signal of stained areas was estimated by light microscopy, based on 25 percentiles in a representative field. Scores were calculated as weighted averages (sum of points × area%). Averages of three independent measurements were calculated to the first decimal place and used for statistical analysis. Observers were not aware of case numbers.

siRNA treatment and cell proliferation assay

Specific siRNA oligonucleotides directed against human DDR1 were purchased from Invitrogen. The Validated Stealth sequence information is DDR1-#1: 5′-GCUAUGUGGAGAU GGAGUUUGAGUU-3′ and DDR1-#2: 5′-GGCCCUGG UUACUCUUCAGCGAAAU-3′. siRNAs were introduced into glioma cell lines by cytofectin-mediated transfection according to the manufacturer's instructions (Qiagen, Tokyo, Japan). Cells were cultured in 96-well plates in 100 μl of serum-enriched medium. When 80% confluence was reached, 25 μl 100 nM siRNA in cytofectin was added drop wise to the cell culture. Numbers of viable cells were evaluated 48 h after culture, by incubating with Tetra color one (Seikagaku CO., Tokyo, Japan), and numbers obtained were compared with those of controls. Control experiments were performed using Cy3-labeled siRNA (Qiagen) directed against an unrelated mRNA (Luciferase; $siRNA_{LUC}$: Qiagen). Transfection efficiency was confirmed with Cy3-labeled $siRNA_{LUC}$ in each assay. All proliferation experiments were repeated as independent experiments at least twice. Results were reported as means ± s.d. of two independent experiments.

Cell invasion of Matrigel

A Transwell containing an 8-μm diameter pore membrane (Becton-Dickinson, Tokyo, Japan) was coated with 500 μl Matrigel (Becton-Dickinson) at 100 μg/ml. Cells were either left untreated, treated with control or DDR1-#1, #2 siRNAs and transfected as described above. After 24-h incubation, cells were detached with cell dissociation solution (Sigma), washed twice with PBS and resuspended in minimum essential medium (MEM) (Nissui Pharmaceutical Inc., Tokyo, Japan) containing 10% fetal bovine serum (FBS) (Gibco, Tokyo, Japan). When siRNAs were used, a second transfection 24 h after the first was performed. In all cases, 2×10^5 cells were seeded into the upper, Matrigel-coated chamber of the Transwell. The lower chamber was filled with MEM supplemented with 10% FBS. After 24-h incubation at 37°C, the non-migrating cells in the upper chamber were gently detached by scraping and adherent cells present on the lower surface of each insert were stained with Giemsa. Ten fields were counted by light microscopy at × 200 magnification. Results were calculated with reference to control values observed after incubation of untreated control, for control and DDR1 siRNA.

Cell lines and culture

All glioma cell lines were cultured in MEM supplemented with 10% FBS. The T98G, GI-1 and U251 cell lines were purchased from Cell Bank, RIKEN BioResource Center (Tsukuba, Japan).

Abbreviations

ALCAM, activated leukocyte cell adhesion molecule; cDNA, complementary DNA; Cy, cyanine; DDR1, discoidin domain receptor family, member 1; DYRK3, dual-specificity tyrosine-(Y)-phosphorylation-regulated kinase 3; FBS, fetal bovine serum; ITGA5, integrin alpha 5; ITGB2, integrin beta 2; KSP37, Ksp37 protein; LDHC, lactate dehydrogenase C; LOC340371, hypothetical protein LOC340371; MEM, minimum essential medium; PBS, phosphate-buffered saline; SLC2A3, solute carrier family 2 member 3; SLN, sarcolipin; s.d., standard deviation; siRNA, short interfering RNA.

Acknowledgements

We are grateful to N Kiyama and F Higuchi for their excellent technical assistance. We thank Dr Rich Simon and Amy Peng for providing the BRB ArrayTools software. The free software was very useful and developed for user-friendly applications. We also thank Tetsutaro Hamano for statistical advices and analysis.

References

Agrawal D, Chen T, Irby R, Quackenbush J, Chambers AF, Szabo M *et al.* (2002). *J Natl Cancer Inst* **94**: 513–521.

Freije WA, Castro-Vargas FE, Fang Z, Horvath S, Cloughesy T, Liau LM *et al.* (2004). *Cancer Res* **64**: 6503–6510.

Godard S, Getz G, Delorenzi M, Farmer P, Kobayashi H, Desbaillets I *et al.* (2003). *Cancer Res* **63**: 6613–6625.

Hoelzinger DB, Mariani L, Weis J, Woyke T, Berens TJ, McDonough WS *et al.* (2005). *Neoplasia* **7**: 7–16.

Hunter SB, Brat DJ, Olson JJ, Von Deimling A, Zhou W, Van Meir EG. (2003). *Int J Oncol* **23**: 857–869.

Karpeh MS, Kelsen DP, Tepper JE. (2001) In: Devita Jr VT (ed) *Cancer of the Stomach: Cancer, Principles & Practice of Oncology*, 6th edn. Lippincott Williams & Wilkins: Philadelphia, pp 1092–1121.

Khan J, Wei JS, Ringner M, Saal LH, Ladanyi M, Westermann F *et al.* (2001). *Nat Med* **7**: 673–679.

Kim S, Dougherty ER, Shmulevich I, Hess KR, Hamilton SR, Trent JM *et al.* (2002). *Mol Cancer Ther* **1**: 1229–1236.

Kleihues P, Cavenee WK. (2000). *World Health Organization Classification of Tumours of the Nervous System.* WHO/IARC: Lyon, France.

Li K, Zhao S, Karur V, Wojchowski DM. (2002). *J Biol Chem* **277**: 47052–47060.

Liang Y, Diehn M, Watson N, Bollen AW, Aldape KD, Nicholas MK *et al.* (2005). *Proc Natl Acad Sci USA* **102**: 5814–5819.

Mischel PS, Cloughesy TF, Nelson SF. (2004). *Nat Rev Neurosci* **5**: 782–792.

Mischel PS, Shai R, Shi T, Horvath S, Lu KV, Choe G *et al.* (2003). *Oncogene* **22**: 2361–2373.

Nigro JM, Misra A, Zhang L, Smirnov I, Colman H, Griffin C *et al.* (2005). *Cancer Res* **65**: 1678–1686.

Nutt CL, Mani DR, Betensky RA, Tamayo P, Cairncross JG, Ladd C *et al.* (2003). *Cancer Res* **63**: 1602–1607.

Ogawa K, Tanaka K, Ishii A, Nakamura Y, Kondo S, Sugamura K *et al.* (2001). *J Immunol* **166**: 6404–6412.

Ramaswamy S, Tamayo P, Rifkin R, Mukherjee S, Yeang CH, Angelo M *et al.* (2001). *Proc Natl Acad Sci USA* **98**: 15149–15154.

Ram R, Lorente G, Nikolich K, Urfer R, Foehr E, Nagavarapu U. (2006). *J Neurooncol* **76**: 239–248.

Rickman DS, Bobek MP, Misek DE, Kuick R, Blaivas M, Kurnit DM *et al.* (2001). *Cancer Res* **61**: 6885–6891.

Rich JN, Hans C, Jones B, Iversen ES, McLendon RE, Rasheed BK *et al.* (2005). *Cancer Res* **65**: 4051–4058.

Sallinen SL, Sallinen PK, Haapasalo HK, Helin HJ, Helen PT, Schraml P *et al.* (2000). *Cancer Res* **60**: 6617–6622.

Shai R, Shi T, Kremen TJ, Horvath S, Liau LM, Cloughesy TF *et al.* (2003). *Oncogene* **22**: 4918–4923.

Sorlie T, Tibshirani R, Parker J, Hastie T, Marron JS, Nobel A *et al.* (2003). *Proc Natl Acad Sci USA* **100**: 8418–8423.

Somasundaram K, Reddy SP, Vinnakota K, Britto R, Subbarayan M, Nambiar S *et al.* (2005). *Oncogene* **24**: 7073–7083.

Stewart LA. (2002). *Lancet* **359**: 1011–1018.

Stupp R, Mason WP, van den Bent MJ, Weller M, Fisher B, Taphoorn MJ *et al.* (2005). *N Engl J Med* **352**: 987–996.

van de Vijver MJ, He YD, van't Veer LJ, Dai H, Hart AA, Voskuil DW *et al.* (2002). *N Engl J Med* **347**: 1999–2009.

van't Veer LJ, Dai H, van de Vijver MJ, He YD, Hart AA, Mao M *et al.* (2002). *Nature* **415**: 530–536.

van den Boom J, Wolter M, Kuick R, Misek DE, Youkilis AS, Wechsler DS *et al.* (2003). *Am J Pathol* **163**: 1033–1043.

Vogel W. (1999). *FASEB J* **13**: S77–82.

Vogel W, Brakebusch C, Fassler R, Alves F, Ruggiero F, Pawson T. (2000). *J Biol Chem* **275**: 5779–5784.

Weiner HL, Zagzag D. (2000). *Cancer Invest* **18**: 544–554.

Wong KK, Chang YM, Tsang YT, Perlaky L, Su J, Adesina A *et al.* (2005). *Cancer Res* **65**: 76–84.

Yoshimura T, Matsuyama W, Kamohara H. (2005). *Immunol Res* **31**: 219–230.

Bioelectromagnetics 27:51–57 (2006)

DNA Strand Breaks Are Not Induced in Human Cells Exposed to 2.1425 GHz Band CW and W-CDMA Modulated Radiofrequency Fields Allocated to Mobile Radio Base Stations

N. Sakuma,[1] Y. Komatsubara,[1] H. Takeda,[1] H. Hirose,[1]* M. Sekijima,[1] T. Nojima,[2] and J. Miyakoshi[3]

[1]*Research Division for Advanced Technology, Kashima Laboratory, Mitsubishi Chemical Safety Institute Ltd., Kamisu, Ibaraki, Japan*
[2]*Division of Electronics and Information Engineering, Graduate School of Hokkaido University, Sapporo, Japan*
[3]*Department of Radiological Technology School of Health Sciences, Faculty of Medicine, Hirosaki University, Hirosaki, Japan*

We conducted a large-scale in vitro study focused on the effects of low level radiofrequency (RF) fields from mobile radio base stations employing the International Mobile Telecommunication 2000 (IMT-2000) cellular system in order to test the hypothesis that modulated RF fields may act as a DNA damaging agent. First, we evaluated the responses of human cells to microwave exposure at a specific absorption rate (SAR) of 80 mW/kg, which corresponds to the limit of the average whole body SAR for general public exposure defined as a basic restriction in the International Commission on Non-Ionizing Radiation Protection (ICNIRP) guidelines. Second, we investigated whether continuous wave (CW) and Wideband Code Division Multiple Access (W-CDMA) modulated signal RF fields at 2.1425 GHz induced different levels of DNA damage. Human glioblastoma A172 cells and normal human IMR-90 fibroblasts from fetal lungs were exposed to mobile communication frequency radiation to investigate whether such exposure produced DNA strand breaks in cell culture. A172 cells were exposed to W-CDMA radiation at SARs of 80, 250, and 800 mW/kg and CW radiation at 80 mW/kg for 2 and 24 h, while IMR-90 cells were exposed to both W-CDMA and CW radiations at a SAR of 80 mW/kg for the same time periods. Under the same RF field exposure conditions, no significant differences in the DNA strand breaks were observed between the test groups exposed to W-CDMA or CW radiation and the sham exposed negative controls, as evaluated immediately after the exposure periods by alkaline comet assays. Our results confirm that low level exposures do not act as a genotoxicant up to a SAR of 800 mW/kg. Bioelectromagnetics 27:51–57, 2006. © 2005 Wiley-Liss, Inc.

Key words: DNA damage; radiofrequency radiation; alkaline comet assay; A172 cells; IMR-90 fibroblasts

INTRODUCTION

The rapid introduction of mobile telecommunication services over the last decade has drastically increased the amount of radiofrequency (RF) field irradiation frequencies and energies in our living environment. In order to continue stable growth and expansion of RF utilizations, it is necessary to investigate the possibility of any biological health effects of RF fields and to obtain reliable confirmation data with respect to safety. To achieve this, animal and cell culture studies of genotoxicity and carcinogenesis are very useful for providing risk assessment information. It is also important to examine the possible biological

Grant sponsor: NTT DoCoMo, Inc.

*Correspondence to: Hideki Hirose, Kashima Laboratory, Mitsubishi Chemical Safety Institute Ltd., 14 Sunayama, Kamisu, Ibaraki 314-0255, Japan. E-mail: h-hirose@ankaken.co.jp

Received for review 15 February 2005; Final revision received 11 July 2005

DOI 10.1002/bem.20179
Published online 10 November 2005 in Wiley InterScience (www.interscience.wiley.com).

© 2005 Wiley-Liss, Inc.

effects of and obtain reliable data for 2-GHz band RF irradiation to facilitate the smooth deployment of the International Mobile Telecommunication 2000 (IMT-2000) cellular system. Here, we conducted a study that focused on the effects of a practical modulated signal for Wideband Code Division Multiple Access (W-CDMA) as well as a continuous wave (CW) at 2.1425 GHz, which corresponds to the middle frequency allocated to the downlink band of IMT-2000 from mobile radio base stations.

To date, most research has concentrated on the biological effects of the relatively high and short period RF irradiation from radio terminals. In contrast, only a few biological experiments related to the low level and long term exposure from radio base stations have been performed, since this exposure level is considered to be too small to have any biological effects on the humans. Moreover, in vitro studies using the single-cell gel electrophoresis (SCG) assay (comet assay), a sensitive technique for detecting DNA strand breaks [Singh et al., 1994, 1995; Tice et al., 2000], reported that RF fields did not induce direct genotoxic or carcinogenic effects [Malyapa et al., 1997; Vijayalaxmi et al., 2000; Li et al., 2001; McNamee et al., 2002a,b, 2003; Hook et al., 2004]. However, Phillips et al. [1998] reported that exposure of Molt-4 T-lymphoblastoid cells to an 836.55 MHz time-division multiple-access (TDMA) signal and 813.5625 MHz iDEN® signal at a specific absorption rate (SAR) of 2.4 mW/kg significantly decreased DNA damage, whereas the same iDEN signal at a SAR of 24 mW/kg significantly increased DNA damage. In addition, Lai and Singh [1995, 1996, 1997] reported that 2450 MHz pulsed and continuous microwave exposure at an average whole body SAR of 1.2 W/kg increased DNA damage in rat brain cells in vivo. Thus, it remains uncertain whether RF fields induce DNA damage, despite the large number of published studies regarding DNA damage after exposure to RF fields.

In the present study, human glioblastoma A172 cells were exposed to W-CDMA radiation at SARs of 80, 250, and 800 mW/kg and CW radiation at 80 mW/kg for 2 and 24 h, while normal human IMR-90 fibroblasts were exposed to both W-CDMA and CW radiations at a SAR of 80 mW/kg for the same time periods. The first objective of this study was to evaluate the responses of these human cells to microwave exposure at a SAR of 80 mW/kg, which corresponds to the limit of the average whole body SAR for general public exposure defined as a basic restriction in the International Commission on Non-Ionizing Radiation Protection [ICNIRP, 1998] guidelines. The second objective was to investigate whether CW and W-CDMA modulated signal RF fields at 2.1425 GHz, which corresponds to the center frequency of the IMT-2000, induced different levels of DNA damage.

MATERIALS AND METHODS

Cells and Culture Conditions

Human glioblastoma A172 cells were cultured in Dulbecco's modified Eagle medium (DMEM; Invitrogen, Tokyo, Japan) supplemented with 10% heat-inactivated fetal calf serum (FCS; Invitrogen), 100 U/ml penicillin, and 100 μg/ml streptomycin. Normal human IMR-90 fibroblasts from fetal lungs were grown in Eagle's minimal essential medium with Earle's balanced salts (Invitrogen) supplemented with 0.1 mM non-essential amino acids, 1.0 mM sodium pyruvate, 10% heat-inactivated FCS, 100 U/ml penicillin, and 100 μg/ml streptomycin. The two cell lines were obtained from the American Type Culture Collection (ATCC, Rockville, MD). All cell cultures were carried out in 100 mm diameter dishes at 37 °C in a humidified atmosphere of 5% CO_2. The doubling times of A172 and IMR-90 cells were 25.4 ± 2.1 and 38.9 ± 3.3 h, respectively, under these culture conditions.

Exposure System

The W-CDMA cellular system is one of the component systems of the IMT-2000 cellular system, and its frequency spectrum is shown in Figure 1. W-CDMA adopts Direct Sequence CDMA (DS-CDMA) and Frequency Division Duplex (FDD) as a multiple access and duplex scheme, respectively. The chip rate of the spread code of this system is 3.84 Mcps. A beam-formed RF exposure incubator employing a horn antenna, a dielectric lens, and a culture case in an anechoic chamber was developed for large-scale in vitro

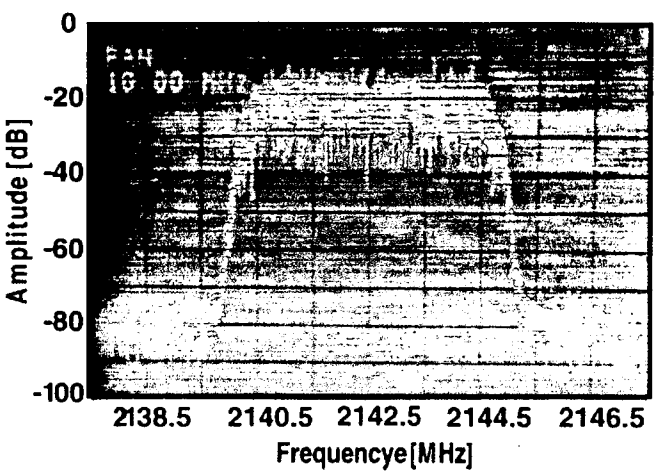

Fig. 1. Wideband Code Division Multiple Access (W-CDMA) frequency spectrum.

studies. A detailed description of the exposure system was published in Iyama et al. [2004]. Briefly, two identical RF field exposure incubators, one for RF field exposure and the other for sham exposure, were established in separate anechoic chambers, and a mechanical switch in a dummy box allows the selection of RF field exposure or sham exposure. This system allows simultaneous exposure of 49 (7 × 7 array) 35 mm culture dishes to a 2.1425 GHz RF electromagnetic field, which corresponds to the center frequency of the IMT-2000 down link band, with a uniform SAR distribution in the medium of all 49 culture dishes. The main unit for the cell exposure provides identical air to the two culture units through sealed ducts at the appropriate temperature (37 °C), CO_2 (5%), and humidity (>90%). The mean SAR of the culture fluid at the bottom of the 49 culture dishes used in the in vitro experiments was 175 mW/kg for an antenna input power of 1 W and the standard deviation of the SAR distribution was 59%. When only the inner 25 culture dishes (5 × 5 array) were evaluated, the mean SAR was 139 mW/kg for the same antenna input power and the standard deviation of the SAR distribution was 47%. Five dishes in the inner dish positions were used in this study.

Experimental Design

Human glioblastoma A172 cells were exposed to W-CDMA radiation at SARs of 80, 250, and 800 mW/kg and CW radiation at 80 mW/kg for 2 and 24 h, while human IMR-90 fibroblasts from fetal lungs were exposed to both W-CDMA and CW radiations at a SAR of 80 mW/kg for the same time periods. The exposure time of 2 and 24 h were chosen because DNA strand breaks increased in a time-dependent manner upon methyl methane sulfonate (MMS) treatment in our preliminary studies (data not shown). A172 glioblastoma or IMR-90 fibroblast cell cultures for RF field exposures were maintained in several 100 mm culture dishes from a common culture. Log phase cells were dissociated enzymatically, plated in 35 mm culture dishes and maintained for 48 h as a pre-culture. Next, the medium was exchanged for fresh medium, and the cell cultures were placed in the RF field exposure incubators. Five cultures were subjected to RF field or sham exposure for 2 or 24 h, respectively. The RF field exposures were processed in a blind manner. The air temperature was monitored for all cultures during the course of the sham and RF field exposures, and no significant variations were found. Empirical data collected over all the experiments demonstrated that the air temperatures within the cultures during the sham and RF field exposures were typically within 0.3 °C of each other at all times, and were within the range of 37.0 ± 0.5 °C once thermodynamic equilibrium was achieved within the exposure chamber at the highest SAR of 800 mW/kg for W-CDMA radiation. The temperatures of the culture media during the sham and RF field exposures cultures typically remained within 0.3 °C. Specifically, the temperature ranges were 37.0 ± 0.3, 37.0 ± 0.1, and 37.0 ± 0.1 °C at the SARs of 800, 250, and 80 mW/kg for W-CDMA radiation, respectively. Other cultures were treated with 0, 2, 4, and 20 μg/ml MMS as positive controls in a conventional incubator. Furthermore, 20 μg/ml MMS was used as a positive control in every RF field exposure experiment.

Alkaline Comet Assay

After the exposure, the RF field, sham and 20 μg/ml MMS samples were processed for the alkaline comet assay as described by Singh et al. [1994, 1995]. Briefly, the cells were washed, resuspended in Ca^{2+}- and Mg^{2+}-free phosphate buffered saline at a concentration of 1×10^5 cells/ml, and mixed with 1% low melting point agarose at a ratio of 1:5. The mixtures were immediately layered onto slides and placed in a refrigerator to allow the mixture to gel. Next, the slides were transferred to a chamber containing lysis buffer (Trevigen, Gaithersburg, MD), and treated with 1 mg/ml proteinase K solution (Qiagen, Tokyo, Japan) at 37 °C for 2 h. The slides were then rinsed in electrophoresis buffer (pH 13; 300 mM NaOH, 1 mM EDTA) for 10 min, subjected to electrophoresis at 22 V and 300 mA for 30 min, dehydrated in 70% ethanol for 10 min and air dried overnight.

The samples were analyzed after staining with 10 μg/ml ethidium bromide. Images were acquired with an Olympus fluorescence microscope using a 20× objective lens and 520–540 nm excitation from a 100 W mercury lamp. All comet images were acquired with a cooled color CCD camera, and at least 100 comets from each of the five replicate cultures were analyzed using the Komet 5 imaging system (Kinetic Imaging Ltd., NC). The comet head and tail regions were defined manually. Tail length was defined as the distance from the leading edge of the comet head to the leading edge of the tail. Tail DNA was calculated as the relative fluorescence intensity in the comet tail region to that in the entire comet. Olive tail moment was calculated as the tail DNA multiplied by the distance between the centers of gravity of the head and tail regions [Olive et al., 1990].

Statistical Analysis

The DNA strand breaks obtained with the alkaline comet assay were analyzed by Student's *t*-test or Welch's *t*-test using the data for the sham exposed samples, the RF field exposed samples and the positive

(20 μg/ml MMS treatment) controls for each of the three end points (Olive tail moment, tail DNA, and tail length). Student's *t*-test was performed if the variance was homogeneous, while Welch's *t*-test was used if the variance was heterogeneous. A *P*-value of less than .05 was considered statistically significant.

RESULTS

DNA Strand Breaks After MMS Treatment

MMS treatment was used as both a positive control and to assess the sensitivity of the method used to detect DNA damage. A172 and IMR-90 cells were cultured with MMS at concentrations of 0, 2, 4, and 20 μg/ml for 2 or 24 h. The lowest detectable dose of each parameter (Olive tail moment, tail DNA, or tail length) was 2 or 4 μg/ml MMS for both cell lines used in the study (Fig. 2). For A172 cells, the Olive tail moment and tail length after culture with 2 μg/ml MMS for 2 h were greater than the background (0 μg/ml MMS), but the difference was not significant. For IMR-90 cells, the tail length after culture with 2 μg/ml MMS for 24 h did not differ significantly from the background (0 μg/ml MMS).

DNA Strand Breaks After Exposure to RF Field at 80 mW/kg

A172 cell cultures were exposed to W-CDMA or CW radiation at a SAR of 80 mW/kg for 2 or 24 h. Experiments under the same RF field exposure conditions were repeated three times, and five different cultures were used in each experiment. The pooled experimental data (15 different cultures) for the same system and duration of RF field exposure are summarized in Table 1. No significant differences were observed between any of the RF field exposure groups and the sham exposed controls for any of the parameters examined, in either the 2.1425 GHz W-CDMA or CW RF field experiments. MMS, the positive control agent, induced a significant and noticeable increase in DNA migration in all experiments.

IMR-90 cells were exposed to W-CDMA or CW radiation at a SAR of 80 mW/kg for 2 or 24 h, and the results are summarized in Table 2. All the comet parameters were small in these experiments. No statistically significant differences were observed between any of the RF field exposure groups and the sham exposed controls for any of the parameters examined, in

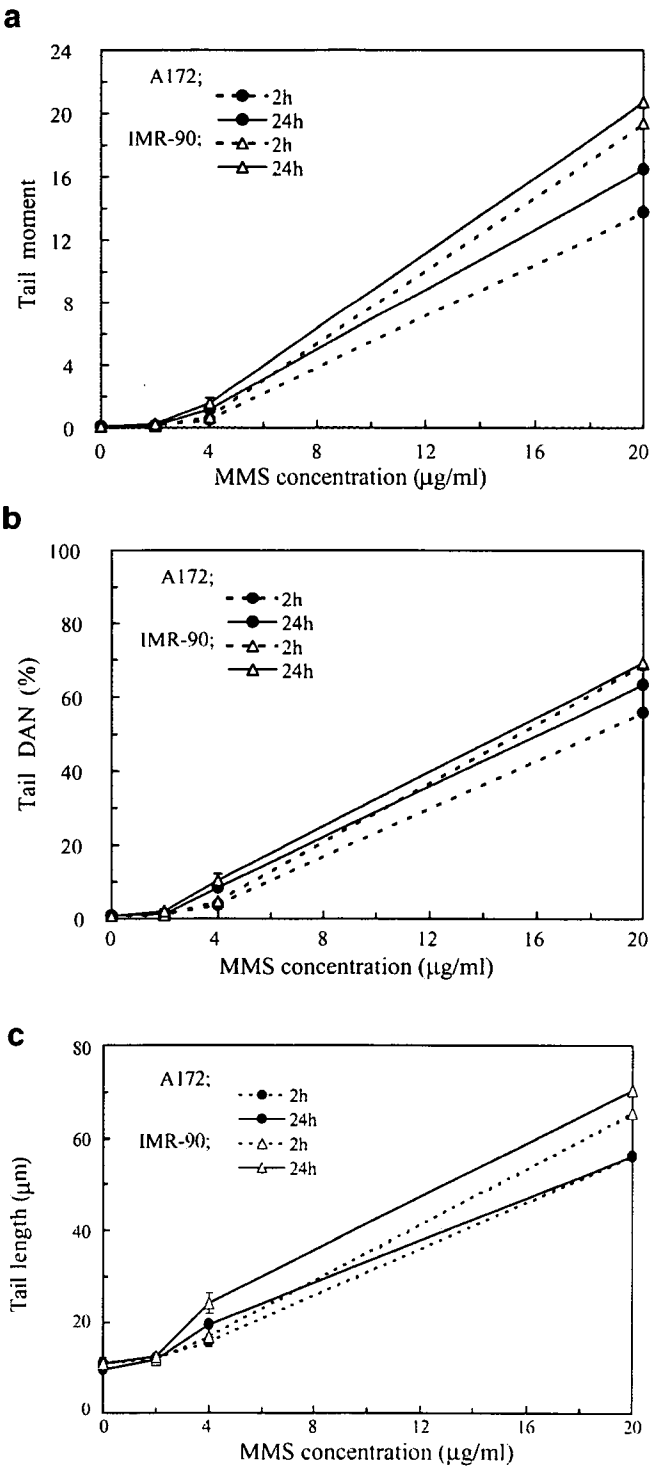

Fig. 2. DNA strand breaks in A172 and IMR-90 cells cultured with methyl methane sulfonate (MMS) at 0, 2, 4, and 20 μg/ml for 2 or 24 h. The Olive tail moment (**a**), tail DNA (**b**), and tail length (**c**) were measured immediately after the treatment. The data points represent the means ± SD of three independent cultures. After treatment of A172 cells with 2 μg/ml MMS for 2 h, the tail moment and tail length are not significantly different from the background (0 μg/ml MMS). However, all three comet parameters differ significantly from the background after treatment with 4 μg/ml MMS ($P < .01$). After treatment of IMR-90 cells with 2 μg/ml MMS for 24 h, the tail length is not significantly different from the background. However, all three comet parameters differ significantly from the background after treatment with 4 μg/ml MMS ($P < .01$).

TABLE 1. Comparison of Comet Parameters in A172 Cells Exposed to 2.1425 GHz Radiofrequency (RF) Radiation and Sham Radiation

System	Specific absorption rate (SAR) (mW/kg)	Time (h)	Tail moment		Tail DNA (%)		Tail length (μm)	
			RF	Sham	RF	Sham	RF	Sham
Wideband Code Division Multiple Access (W-CDMA)	800	2	0.20 ± 0.060	0.19 ± 0.060	1.71 ± 0.525	1.64 ± 0.538	11.56 ± 2.112	11.20 ± 2.329
		24	0.16 ± 0.037	0.16 ± 0.031	1.42 ± 0.367	1.42 ± 0.334	11.15 ± 2.223	10.97 ± 2.316
	250	2	0.26 ± 0.063	0.27 ± 0.083	2.23 ± 0.583	2.28 ± 0.685	12.03 ± 1.625	12.04 ± 1.656
		24	0.26 ± 0.059	0.27 ± 0.059	2.30 ± 0.607	2.38 ± 0.632	12.11 ± 1.581	12.21 ± 1.512
	80	2	0.26 ± 0.043	0.27 ± 0.029	2.28 ± 0.341	2.33 ± 0.241	13.36 ± 1.276	13.25 ± 1.645
		24	0.27 ± 0.050	0.29 ± 0.054	2.38 ± 0.432	2.50 ± 0.358	13.29 ± 1.426	13.29 ± 1.559
Continuous wave (CW)	80	2	0.24 ± 0.168	0.23 ± 0.150	2.10 ± 1.636	2.01 ± 1.407	10.07 ± 3.097	9.93 ± 3.226
		24	0.25 ± 0.174	0.24 ± 0.167	2.24 ± 1.725	2.14 ± 1.672	10.34 ± 2.701	9.92 ± 3.116
MMS[a]		2	—	16.31 ± 5.095*	—	62.32 ± 8.664*	—	49.44 ± 9.859*
		24	—	19.44 ± 4.752*	—	67.65 ± 7.889*	—	53.51 ± 8.120*

Each data point represents the mean ± the standard deviation (SD) for 15 cultures. One hundred cells (50 cells from two spots) were measured for each culture at each experiment.
[a]Other cultures were treated with 20 μg/ml methyl methane sulfonate (MMS) for positive control in every RF exposure experiment; mean ± the SD for three experiments (cultures).
*Significance ($P < .001$) from the sham control.

TABLE 2. Comparison of Comet Parameters in IMR-90 Cells Exposed to 2.1425 GHz RF Radiation and Sham Radiation

System	SAR (mW/kg)	Time (h)	Tail moment		Tail DNA (%)		Tail length (μm)	
			RF	Sham	RF	Sham	RF	Sham
W-CDMA	80	2	0.14 ± 0.076	0.14 ± 0.086	1.35 ± 0.842	1.36 ± 0.894	9.06 ± 3.877	8.89 ± 4.218
		24	0.15 ± 0.139	0.11 ± 0.062	1.38 ± 1.104	1.15 ± 0.653	8.72 ± 4.296	8.16 ± 4.463
CW	80	2	0.09 ± 0.014	0.09 ± 0.015	0.75 ± 0.091	0.76 ± 0.108	7.57 ± 2.446	7.74 ± 2.138
		24	0.09 ± 0.019	0.09 ± 0.017	0.75 ± 0.195	0.77 ± 0.169	7.41 ± 1.522	7.94 ± 1.729
MMS[a]		2	—	17.13 ± 1.519*	—	66.76 ± 3.320*	—	58.44 ± 7.545*
		24	—	19.52 ± 2.665*	—	70.74 ± 3.289*	—	57.75 ± 9.119*

Each data point represents the mean ± the SD for 15 cultures. One hundred cells (50 cells from two spots) were measured for each culture at each experiment.
[a]Other cultures were treated with 20 μg/ml MMS for positive control in every RF exposure experiment; mean ± the SD for three experiments (cultures).
*Significance ($P < .001$) from the sham control.

either the 2.1425 GHz W-CDMA or CW RF field experiments. MMS induced a significant increase in DNA migration in all experiments.

DNA Strand Breaks After Exposure to RF Field at 250 or 800 mW/kg

A172 cell cultures were exposed to W-CDMA radiation at a SAR of 250 or 800 mW/kg for 2 or 24 h, and the results are summarized in Table 1. No significant differences were observed between any of the W-CDMA exposure groups and the sham exposed controls for any of the parameters examined at an average SAR of 250 or 800 mW/kg. MMS induced a significant increase in DNA migration in all experiments.

DISCUSSION

The comet assay is a simple and sensitive assay that is capable of measuring and identifying DNA strand breaks at the cellular level [Singh et al., 1995; Tice et al., 2000]. In both cell lines, treatment with 20 μg/ml MMS for 2 and 24 h induced increases in all three comet parameters (Olive tail moment, tail DNA, and tail length), although the survival of the cells did not differ from the background after either 2 or 24 h of treatment (A172: 2 h, 91.0% vs. 96.0%; 24 h, 91.0% vs. 98.8%; IMR-90: 2 h, 93.7% vs. 96.3%; 24 h, 90.6% vs. 95.9%).

Figure 2 shows the DNA strand breaks in A172 and IMR-90 cells after culture with different concentrations of MMS for 2 or 24 h. In our comet assay protocol, the cell suspensions and low melting point agarose layered onto slides were treated with 1 mg/ml proteinase K to increase the sensitivity, since Singh et al. [1995] reported that proteinase K treatment of cells allowed the detection of DNA strand breaks in human lymphocytes irradiated with low doses of γ rays. Our results further confirmed that proteinase K treatment of the cells raised the sensitivity of detection of DNA strand breaks. None of the measured comet parameters in comet assays for A172 or IMR-90 cells were significantly higher than the background after treatment with 10 μg/ml MMS without proteinase K treatment (data not shown). However, all the comet parameters were significantly above the background after treatment of both cell lines with 4 μg/ml MMS followed by 1 mg/ml proteinase K (Fig. 2). Thus, these results confirmed that the comet assay performed in this study could detect DNA strand breaks with high sensitivity.

In the present study, we analyzed the human A172 and IMR-90 cells for DNA strand breaks after exposure to RF signals for 2 or 24 h. A172 cells were exposed to W-CDMA radiation at SARs of 80, 250, and 800 mW/kg and CW radiation at 80 mW/kg, while IMR-90 cells were exposed to both W-CDMA and CW radiations at a SAR of 80 mW/kg. The exposures to RF radiation were carried out in a blind manner so that it was not possible to identify the RF field and sham exposed samples. Three comet parameters (Olive tail moment, tail DNA, and tail length) were obtained for each comet scored by image analysis, after averaging the responses across different populations of cells within each culture. For all the RF field exposure conditions, no significant differences in the DNA strand breaks were observed between the test groups exposed to W-CDMA or CW radiation and the sham exposed negative controls when the samples were processed immediately after the exposure periods by the alkaline comet assay. In our previous study, we showed that exposure to 2.1425 GHz CW and W-CDMA modulated RF signals at a SAR of up to 800 mW/kg did not alter the cell proliferation ratio or cell cycle phase in four human cell lines, including A172 and IMR-90 cells. Furthermore, none of the CW and W-CDMA modulated RF signals tested had any effects on the expression profiles of genes encoding proteins related to the cell cycle, cell proliferation, cell death, apoptosis, etc. (data not shown).

Our results confirm that exposure to W-CDMA and CW 2.1425 GHz microwaves for 2 and 24 h did not act as a genotoxicant at the limit of the average whole body SAR level defined in the ICNIRP guidelines.

ACKNOWLEDGMENTS

The authors thank Ms. Naoko Kaji for her technical assistance during this research.

REFERENCES

Hook GJ, Zhang P, Lagroye I, Li L, Higashikubo R, Moros EG, Straube WL, Pickard WF, Baty JD, Roti Roti JL. 2004. Measurement of DNA damage and apoptosis in Molt-4 cells after in vitro exposure to radiofrequency radiation. Radiat Res 161:193–200.

ICNIRP. 1998. Guidelines for limiting exposure to time varying electric, magnetic and electromagnetic fields (up to 300 GHz). Health Phys 74:494–522.

Iyama T, Ebara H, Tarusawa Y, Uebayashi S, Sekijima M, Nojima T, Miyakoshi J. 2004. Large-scale in vitro experiment system for 2 GHz-exposure. Bioelectromagnetics 25:599–606.

Lai H, Singh NP. 1995. Acute low-intensity microwave exposure increases DNA single-strand breaks in rat brain cells. Bioelectromagnetics 16:207–210.

Lai H, Singh NP. 1996. Single- and double-strand DNA breaks in rat brain cells after acute exposure to radiofrequency electromagnetic radiation. Int J Radiat Biol 69:513–521.

Lai H, Singh NP. 1997. Melatonin and a spin-trap compound block radiofrequency electromagnetic radiation-induced DNA strand breaks in rat brain cells. Bioelectromagnetics 18: 446–454.

Li L, Bisht KS, LaGroye I, Zhang P, Straube WL, Moros EG, Roti Roti JL. 2001. Measurement of DNA damage in mammalian cells exposed in vitro to radiofrequency fields at SARs of 3–5 W/kg. Radiat Res 156:328–332.

Malyapa RS, Ahern EW, Straube WL, Moros EG, Pickard WF, Roti Roti JL. 1997. Measurement of DNA damage after exposure to electromagnetic radiation in the cellular phone communication frequency band (835.62 and 847.74 MHz). Radiat Res 148:618–627.

McNamee JP, Bellier PV, Gajda GB, Miller SM, Lemay EP, Lavallee BF, Marro L, Thansandote A. 2002a. DNA damage and micronucleus induction in human leukocytes after acute in vitro exposure to a 1.9 GHz continuous-wave radiofrequency field. Radiat Res 158:523–533.

McNamee JP, Bellier PV, Gajda GB, Lavallee BF, Lemay EP, Marro L, Thansandote A. 2002b. DNA damage in human leukocytes after acute in vitro exposure to a 1.9 GHz pulse-modulated radiofrequency field. Radiat Res 158:534–537.

McNamee JP, Bellier PV, Gajda GB, Lavallee BF, Marro L, Lemay EP, Thansandote A. 2003. No evidence for genotoxic effects from 24 h exposure of human leukocytes to 1.9 GHz radiofrequency fields. Radiat Res 159:693–697.

Olive PL, Banath JP, Durand RE. 1990. Heterogeneity in radiation-induced DNA damage and repair in tumor and normal cells using the "comet" assay. Radiat Res 122:86–94.

Phillips JL, Ivaschuk O, Ishida-Jones T, Jones RA, Compbell-Beachler M, Haggren W. 1998. DNA damage in Molt-4 T-lymphoblastoid cells exposed to cellular telephone radiofrequency fields in vitro. Bioelectrochem Bioenerg 45:103–110.

Singh NP, Stephens RE, Schneider EL. 1994. Modification of alkaline microgel electrophoresis for sensitive detection of DNA damage. Int J Radiat Biol 66:23–28.

Singh NP, Graham MM, Singh V, Khan A. 1995. Induction of DNA single-strand breaks in human lymphocytes by low dose of γ-rays. Int J Radiat Biol 68:563–569.

Tice RR, Agurell E, Anderson D, Burlinson B, Hartmann A, Kobayashi H, Miyamae Y, Rojas E, Ryu JC, Sasaki YF. 2000. Single cell gel/comet assay: Guidelines for in vitro and in vivo genetic toxicology testing. Environ Mol Mutagen 35: 206–221.

Vijayalaxmi, Leal BZ, Szilagyi M, Prihoda TJ, Meltz ML. 2000. Primary DNA damage in human blood lymphocytes exposed in vitro to 2450 MHz radiofrequency radiation. Radiat Res 153:479–486.

Skeletal Radiol (2006) 35: 543–546
DOI 10.1007/s00256-005-0037-5

CASE REPORT

Mototaka Miyake
Ukihide Tateishi
Tetsuo Maeda
Yasuaki Arai
Kunihiko Seki
Tadashi Hasegawa
Kazuro Sugimura

Sclerosing perineurioma: tumor of the hand with a short T2

Received: 2 June 2005
Revised: 17 August 2005
Accepted: 17 August 2005
Published online: 19 October 2005
© ISS 2005

M. Miyake · U. Tateishi (✉) ·
T. Maeda · Y. Arai
Division of Diagnostic Radiology
and Nuclear Medicine,
National Cancer Center Hospital,
5-1-1, Tsukiji, Chuo-ku,
104-0045 Tokyo, Japan
e-mail: utateish@ncc.go.jp
Tel.: +81-3-35422511
Fax: +81-3-35423815

K. Seki
Division of Pathology,
National Cancer Center Hospital,
Tokyo, Japan

T. Hasegawa
Department of Clinical Pathology,
Sapporo Medical University
School of Medicine,
Sapporo, Japan

K. Sugimura
Department of Radiology,
Kobe University Graduate
School of Medicine,
Kobe, Japan

Abstract We present two cases of sclerosing perineurioma, a rare soft tissue tumor, in the palm and the ring finger respectively, presenting as a small, painless and subcutaneous mass. This tumor has a predilection for the digits and palms of young, predominantly male adults. In the present cases the tumors showed very low signal intensity on T2-weighted magnetic resonance (MR) images. Histologically they contained abundant collagen and hyalinized stroma, which would account for areas of low signal intensity on T2-weighted MR images. Immunohistochemically, the tumor cells were positive for vimentin, epithelial membrane antigen and human erythrocyte glucose transporter 1 and negative for S-100 protein. To the best of our knowledge, the appearance of sclerosing perineurioma on MR imaging has not been previously reported in the English-language literature. Sclerosing perineurioma should be considered in the differential diagnosis of hand tumors when the tumor shows low signal intensity on T2-weighted MR images.

Keywords Sclerosing perineurioma · Hand · MRI · Short T2

Introduction

Perineurioma is a rare soft tissue tumor composed of cells resembling those of the normal perineurium. It was first described in 1978 by Lazarus and Trombetta on the basis of ultrastructural findings [1]. There are two distinct forms of perineurioma, the intraneural and the extraneural; the latter is known as soft tissue perineurioma. Sclerosing perineurioma, first described by Fetsch and Miettinen in 1997, is an unusual variant of soft tissue perineurioma that presents as a small, painless, dermal or subcutaneous mass with a strong predilection for the digits and palms of young adults, predominantly males [2]. To the best of our knowledge, the appearance on magnetic resonance imaging (MRI) of sclerosing perineurioma has not been previously reported in the English-language literature. We report the MRI features of two cases of sclerosing perineurioma and correlate the MR findings with histological features.

Case report

Case 1

An 11-year-old girl presented with a 1- year history of a slowly growing painless mass in her left palm. Physical examination revealed a well-delineated elastic and hard mass

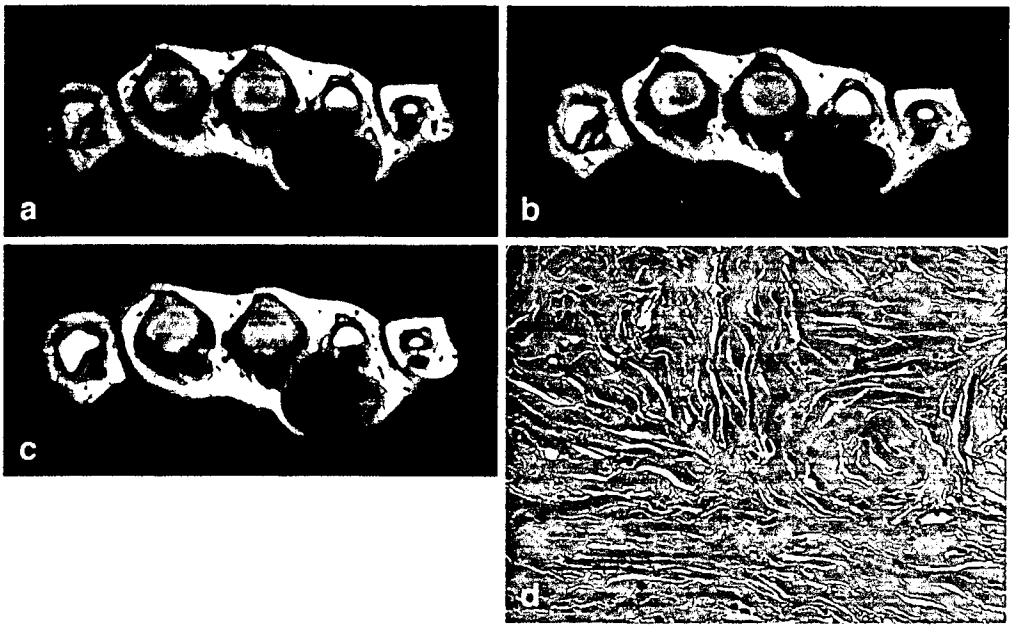

Fig. 1 An 11-year-old girl with a painless mass in her left palm. **a** Axial T1-weighted SE MR image (TR/TE 440/25) shows an iso signal intensity mass to that of muscle, in her left palm. **b** Axial T2-weighted FSE MR image (TR/TE 4000/87.3) reveals homogenously very low signal intensity of the mass. **c** Axial gadolinium-enhanced T1-weighted SE MR image suppression shows partial enhancement. **d** Photomicrograph of the tumor shows small, oval epithelioid or plump spindle cells, scattered and arranged in a corded and whorled pattern in abundant collagenous background. (H&E, ×40)

in her left palm and no limitation of finger motion. Radiographs showed a soft tissue mass in her left palm without erosion of adjacent bone. MRI of the left hand revealed a well-delineated mass measuring maximally 25×28 mm between the flexor tendons of the middle and ring fingers. The mass appeared homogeneous with signal intensity similar to that of muscle on T1-weighted spin echo (SE) MR images (Fig. 1a). On T2-weighted fast spin echo (FSE) MR images, the mass showed homogeneous low signal intensity similar to that of the tendons (Fig. 1b). On gadolinium-enhanced T1-weighted SE MR images with fat suppression, the mass showed partial slight enhancement (Fig. 1c). The margin of the mass displayed low signal intensity on all MRI pulse sequences, suggestive of a capsule or pseudocapsule. An excisional biopsy was performed. Grossly, the tumor was firm, well circumscribed and surrounded by a thin fibrous pseudocapsule. The cut surface of the tumor was solid, whitish and homogeneous in appearance.

Histologic examination revealed abundant collagenous tissue and small, oval epithelioid or plump spindle cells scattered and arranged in a corded, whorled or trabecular pattern (Fig. 1d). Small foci of necrosis, that is, ischemic infarction—possibly as a result of thrombosis—were identified (not shown). Cellular and nuclear atypia was rare and mitoses were not present. Tumor cells were positive for vimentin and epithelial membrane antigen (EMA) and negative for S-100 protein. In addition, they were diffusely and strongly positive for human erythrocyte glucose transporter 1 (GLUT1) with intensity similar to that of erythrocytes in tissue sections. The histological diagnosis of sclerosing perineurioma was made. After simple excision, there has been no evidence of recurrence or metastasis for 4 years, 4 months.

Case 2

A 16-year-old male presented with a painless and firm mass on the palmar side of his left ring finger. The mass slightly limited the range of motion of his ring finger. Laboratory tests showed no abnormalities. MRI of the left hand revealed a clearly defined mass measuring maximally 40×25 mm along the flexor tendon of his left ring finger. The lesion showed homogenously low to iso signal intensity relative to muscle on T1-weighted SE MR images (Fig. 2a) and very low signal intensity, similar to the tendons, on T2-weighted FSE MR images (Fig. 2b). On gadolinium-enhanced T1-weighted SE MR images, the lesion showed heterogeneous enhancement (Fig. 2c). On MRI, the tumor was attached to the flexor tendon of the left ring finger and there were no tendinous abnormalities. The patient underwent an excisional biopsy. Although the tumor was exophytically attached to the flexor digitorum profundus tendon of the left ring finger, there was no encasement of the flexor digitorum profundus tendon. The tumor was completely excised and the flexor tendon was preserved. Microscopic examination showed abundant collagen, which was partially sclerosed and hyalinized. In the collagenous background, there were small, oval epithelioid or plump spindle cells scattered and arranged

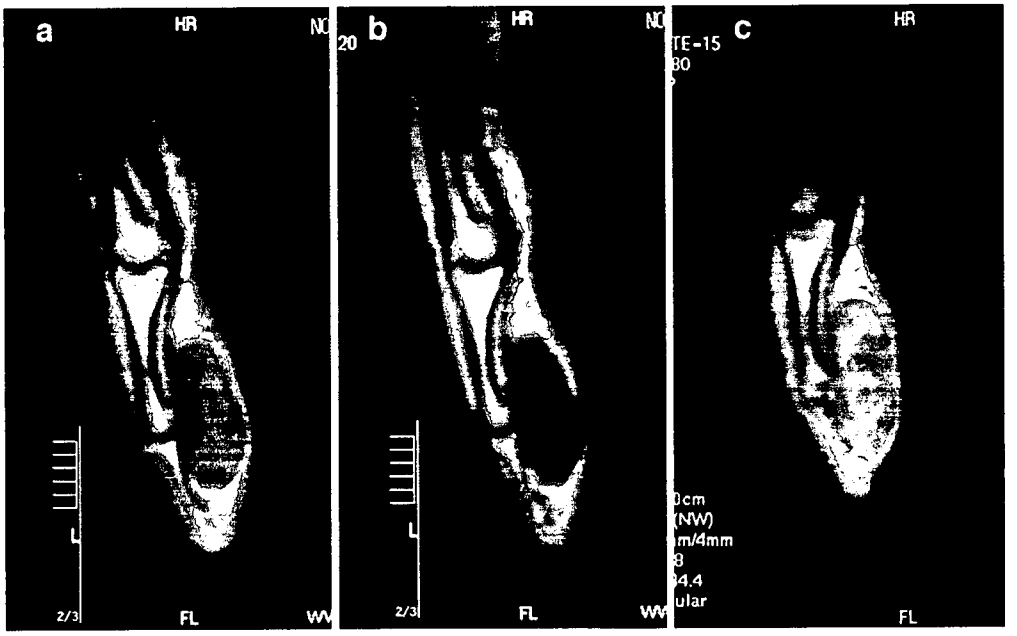

Fig. 2 A 16-year-old male with a painless mass in his left ring finger. **a** Sagittal T1-weighted SE MR image (TR/TE 440/25) shows a low- to iso-signal-intensity mass in comparison with muscle. **b** Sagittal T2-weighted FSE MR image (4500/120) reveals homogeneously very low signal intensity to the mass. **c** Sagittal gadolinium-enhanced T1-weighted SE MR image (500/15) with fat suppression shows heterogeneous enhancement

in a corded, whorled or trabecular pattern. Tumor cells were diffusely and strongly positive for GLUT1 and diffusely positive for vimentin and EMA. These histological findings were consistent with sclerosing perineurioma. On follow-up at 2 years, 2 months, there was no evidence of recurrence or metastasis.

Discussion

Sclerosing perineurioma is a rare soft tissue tumor composed of cells resembling those of the normal perineurium. It presents as a small, painless, dermal or subcutaneous mass with a strong predilection for the digits and palms of young adults [2]. Why this tumor has a marked predilection for the hands of young adults is unknown. The predominant chief complaint is a painless but slowly growing mass, which may range in size from 0.7 cm to 4.0 cm in its maximal dimension [2, 3]. All reported sclerosing perineuriomas have had an excellent course without recurrence or metastasis. Malignant transformation has not been reported. Therefore, local excision is considered adequate therapy.

The diagnosis requires light-microscopic, ultrastructural and immunohistochemical examination. Grossly, the tumor is a well-circumscribed and nodular or ovoid firm mass [2, 4, 5]. Microscopically, the tumor is hypocellular with an extensively collagenized stroma and contains small epithelioid and plump spindle cells showing a characteristic corded or whorled growth pattern [2]. Perineurioma cells immunohistochemically express vimentin and EMA and lack immunoreactivity for S-100 protein [2]. Hirose et al. reported that the expression of GLUT1 was specific to perineurial cells and useful to distinguish perineurial cells from other nerve sheath cells [6]. In our two cases GLUT1 showed strongly positive staining, similar to previous results [3].

Since sclerosing perineurioma is not a widely recognized entity, its features on diagnostic imaging, including MRI, have not been previously reported. In the present cases, the tumors showed signal intensity similar to that of muscle on T1-weighted SE MR images and very low signal intensity on T2-weighted FSE MR images. After gadolinium administration, the lesions were partially enhanced in case 1 and diffusely enhanced in case 2. It is known that areas of low signal intensity on T2-weighted MR images can be seen with hemosiderin deposition or with areas of decreased cellularity and dense collagen deposition [7]. The present tumors histologically contained abundant collagen and hyalinized stroma, which were consistent with areas of low signal intensity on T2-weighted MR images. MRI clearly delineated the depth of the tumor and its relationship to the flexor digitorum profundus tendon, aiding in surgical planning. In each of these cases the tumor was exophytically attached to the flexor digitorum profundus tendon and was surrounded by a thin capsule or pseudocapsule, which was confirmed histologically. In our two cases, GLUT1 was strongly positive immunohistochemically.

On MRI, the differential diagnosis of sclerosing perineurioma includes giant cell tumor of tendon sheath, fibroma, neurofibroma, proliferative fasciitis, myxofibrosarcoma, myxoinflammatory fibroblastic sarcoma and clear cell sarcoma, all of which may show low signal intensity on T2-weighted MR images [7–10].

In summary, we have described the MRI features of two cases of sclerosing perineurioma in the left palm and in the left ring finger of young patients.

Awareness of this rare tumor with a short T2 and a predilection for the digits and palms would prompt the interpreter to include sclerosing perineurioma in the differential diagnosis. An excision with tendon-sparing surgery appears to result in cure.